18th AIAA/CEAS Aeroacoustics Conference (33rd AIAA Aeroacoustics Conference)
04 - 06 June 2012, Colorado Springs, CO

AIAA 2012-2258

Nonlinear Evolution of Noise from a Military Jet Aircraft during Ground Run-up

Kent L. Gee[1]
Brigham Young University, Provo, UT, 84602, USA

J. Micah Downing[2] and Michael M. James[3]
Blue Ridge Research and Consulting, LLC, Asheville, NC, 28801, USA

Robert C. McKinley[4] and Richard L. McKinley[5]
Air Force Research Laboratory, Wright-Patterson Air Force Base, OH,45433, USA

and

Tracianne B. Neilsen[6] and Alan T. Wall[7]
Brigham Young University, Provo, UT, 84602, USA

Nonlinear propagation of noise measured during static run-up measurements of a military jet aircraft is considered. Measurements made of the noise radiation from the F-35AA Joint Strike Fighter indicate levels commensurate with finite-amplitude sound propagation, both through a Gol'dberg number analysis and numerical modeling. Comparisons with a nonlinear propagation model based on the generalized Mendousse-Burgers equation and augmented for weak-shock theory agree favorably with the measurements.

I. Introduction

THE nonlinear propagation of high-amplitude jet noise is a research topic that has received renewed interest during the past decade. For example, experimental studies by Gee *et al*.[1,2] and Petitjean *et al*.[3] were followed by other studies by Viswanathan *et al*.,[4,5] and Greska and Krothapalli[6]. Recently, Gee *et al*.[7] and Baars *et al*.[8] have examined nonlinear effects of fully expanded, model-scale supersonic jet noise using various signal processing

[1] Associate Professor, Department of Physics and Astronomy, N-283 ESC, AIAA Senior Member.
[2] Chief Scientist, 15 W. Walnut St., Suite C.
[3] Senior Pricipal Engineer, 15 W. Walnut St., Suite C.
[4] Senior Research Psychologist, Battlespace Acoustics Branch, AFRL 711 HPW/RHCB
[5] Principal Acoustics Engineer, AFRL 711 HPW/RHCB
[6] Part-time Professor, Department of Physics and Astronomy, N-283 ESC.
[7] PhD Candidate, Department of Physics and Astronomy, N-283 ESC, AIAA Student Member.

[a)] SBIR DATA RIGHTS - (DFARS 252.227-7018 (JUNE 1995)); Contract Number: FA8650-08-C-6843;
Contractor Name & Address: Blue Ridge Research and Consulting, LLC, 15 W Walnut St., Suite C; Asheville, NC
Expiration of SBIR Data Rights Period: March 17, 2016 (Subject to SBA SBIR Directive of September 24, 2002)
The Government's rights to use, modify, reproduce, release, perform, display, or disclose technical data or computer software marked with this legend are restricted during the period shown as provided in paragraph (b)(4) of the Rights in Noncommercial Technical Data and Computer Software—Small Business Innovation Research (SBIR) Program clause contained in the above identified contract. No restrictions apply after the expiration date shown above. Any reproduction of technical data, computer software, or portions thereof marked with this legend must also reproduce the markings.
[b)] Distribution A – Approved for Public Release; Distribution is Unlimited; 88ABW-2012-3048

techniques. The preceding studies have examined various aspects of the complex research problem, but the most direct evidence to date of the significance of nonlinear propagation of jet noise has been a study of the noise propagation from the F-22A Raptor.[9,10] In these studies, nonlinear waveform steepening, and a corresponding transfer of energy upward in the spectrum, was predicted to be significant, which was verified by measurement. With one aircraft engine at afterburner power, nonlinear propagation out to 305 m results in levels at 20 kHz that are approximately 100 dB greater than predicted by linear propagation. Nonlinear effects were found to be present along the full 55° measurement span from the sideline aft of the aircraft, for even intermediate engine conditions.

This paper describes results of a propagation experiment during static tests of the F-35AA Joint Strike Fighter. Given the relative specifications of the F-22A and F-35AA engines, nonlinear effects are also expected to be present. Consequently, a similar approach in terms of comparing measured and modeled far-field spectra is taken. Following a summary of the measurement layout and conditions, and an overview of some of the measured results, measured and predicted spectra are compared.

II. Measurement Summary

The F-35AA static run-up measurements were conducted 18 October, 2008 at Edwards Air Force Base (EAFB), CA. The measurements were made jointly by the Air Force Research Laboratory, Blue Ridge Research and Consulting, and Brigham Young University. A photograph of the tied-down aircraft is displayed in Figure 1.

Figure 1. Tied-down F-35AA aircraft at Edwards Air Force Base. Also visible are some of the tripods of the near-field microphone array.

Microphones were located relative to the aircraft as shown in Figure 2, at a height of 1.52 m (5 ft). Additional microphones were located at 152 m, 305 m, 610 m, and 1220 m (500, 1000, 2000, and 4000 ft, respectively). The layout is illustrated in Ref. 11. Measurements were made using 6.35 mm Type 1 free-field or pressure microphones. The pressure microphones were oriented skyward, for nominally grazing incidence. The free-field microphones were pointed toward the plume, aimed at a point approximately 6.7 m aft of the aircraft. This point, which is about 7 nozzle diameters downstream of the engine exit plane (the same scaled distance used for the F-22 experiment in 2004)[10], was set as the origin for the microphone arcs at 76 m and beyond. The microphone array, coupled with the microphones at greater distances, represent the most spatially extensive measurements of a military jet aircraft to date. Microphones had been originally located closer to the presumed shear layer, but an early-morning cross wind prompted some concerns about microphone security and led to a shift in position. (Note that the wind dissipated shortly after the microphones were moved and the average wind speed during the test was less than 1 kt.)

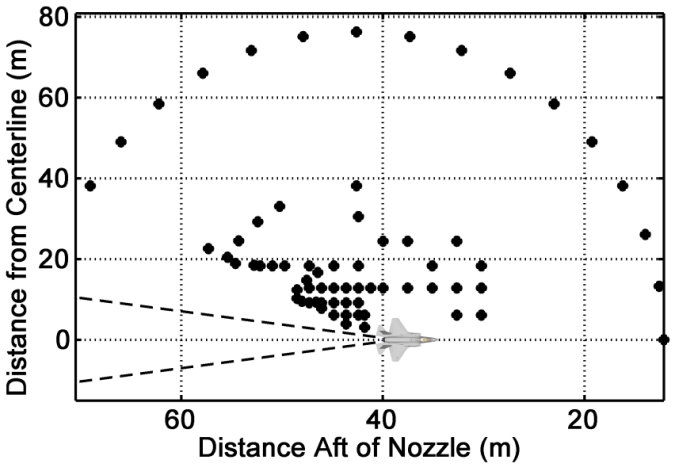

Figure 2. Shematic with dots showing the layout of microphones relative to the aircraft.

During the test, the ambient pressure was virtually constant at 0.914 kPa. Temperature and relative humidity varied from 7 – 16 °C and 21-27%, respectively. Because atmospheric absorption varies considerably as a function of humidity for these relatively dry conditions, it is worthwhile to consider the level change, in decibels, due to atmospheric absorption over a propagation range of 229 m (750 ft). This result is displayed in Figure 3. The results changepredicted levels vary monotonically as a function of temperature and relative humidity; the lowest humidity and temperature produce the most loss in the mid-frequency range (1-3 kHz) and the lowest loss at high frequencies. The variation in level at 20 kHz over the relatively small change in ambient conditions is very large (~70 dB at 20 kHz) and emphasizes the need to collect accurate ambient condition information when examining data for nonlinear propagation effects. It is further noted, however, that these are the losses expected for *linear* propagation, and the effect of the atmosphere on a waveform undergoing significant nonlinear propagation is expected to be different. Nonlinear propagation over the same range as a function of atmospheric conditions is considered further in Section IV.

Figure 4 shows a Google Earth® image of the run-up pad at EAFB, with a superimposed aircraft image at the approximate location during testing. The three radial lines denote three angles measured relative to the engine inlet;to provide scale, the lines are 305 m (1000 ft) in length. Unfortunately, the overall propagation environment was not as "clean" as for the 2004 F-22A measurements in that aft of the aircraft, there was 60-100 m of a moderately dense sagebrush cover, and to the sideline and forward directions, there were both sagebrush and elevation changes.

Data acquisition was carried out using two different setups. The microphones inside the 76 m arc were recorded using a National Instruments® 8353 Raid server connected to a PXI chassis containing 4462 cards. Analog input ranges for each channel were adjusted (in 10 dB increments) based on the sensitivity of each microphone in order to maximize the dynamic range of each of the 24-bit cards. The system sampling frequency was varied between 96 and 204.8 kHz. The lower sampling rate was required because of slower hard drive write speeds for the early-morning tests while the system was cold and during afterburner, where system vibration was greater. The system was located forward of the aircraft and to the sideline (about 70°) at an approximate distance of 35 m. Data from the microphone arc at 76 m was recorded using a separate National Instruments® recording system, also at a sampling rate of 96 kHz. Data were recorded over a variety of engine conditions; however, only data at military (100% ETR) power are discussed here.

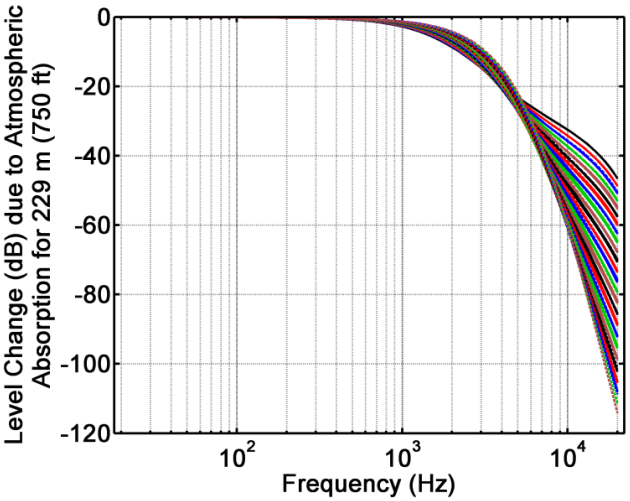

Figure 3. Level change (dB) due to atmospheric absorption losses for increasing temperature and relative humidity at an ambient pressure of 0.914 kPa and a propagation range of 229 m (750 ft), based on linear propagation. At 20 kHz, the top curve (least loss) is for 7 °C and 21% relative humidty and the bottom curve is for 13 °C and 27 °C.

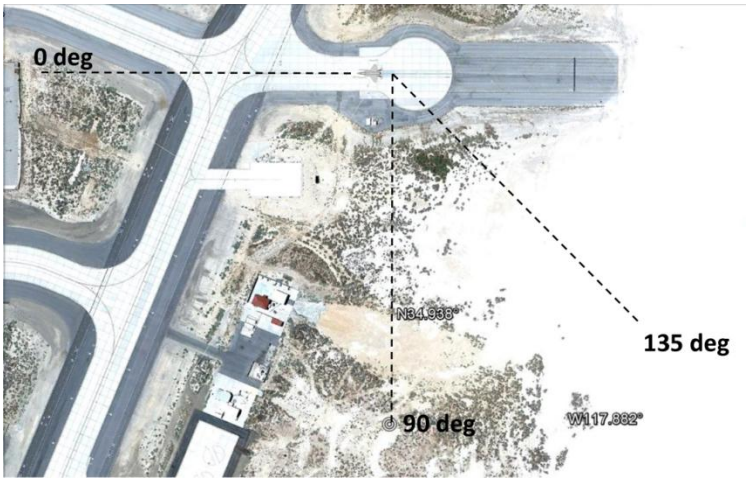

Figure 4. Run-up pad environment at Edwards Air Force Base. The radial lines are 305 m (1000 ft) in length; the origin is located 6.7 m downstream of the nozzle exit.

III. Measurement Results

A. Overall Level Maps

Included in this section are overall level maps at MIL power recorded in the near-field and the 76 m measurement arc. Figure 5 shows an overall sound pressure level (OASPL)map, interpolated between measurement locations (shown as the outlined white circles). The triangulation-based interpolation is performed in MATLAB ® and is not necessarily physical. This is particularly true in the immediate vicinity of the aircraft itself, where no measurements could be made. Extrapolation from the dominant radiation direction (~130°) back in toward the source suggests that the chosen origin (6.7 m-downstream) is an acceptable approximation of the maximum source region. This is in the vicinity of the peak source region predicted for the maximum radiation direction by Schlinker *et al.*[12] The actual measurements in Figure 5 show OASPLs greater than 150 dB re 20 μPa just 1-2 m from the shear layer.

The second map included is intended to help guide others intending to make similar measurements in the future. Although the rms levels in Figure 5 are high, there must be sufficient dynamic range of the data acquisition system to accommodate the peak excursions in the waveform. Gabrielson *et al*.[13] indicated that the peak pressures can be as great as ten times the *rms* pressures in the waveform, which would correspond to a crest factor of 20 dB. Figure 6 shows the measured 99.999th percentile crest factor at all the microphones. Because each recording was on the order of 30 s, basing the crest factor on a single peak value out of nearly three million points seemed inappropriate. Consequently, the 99.999th percentile (or approximately the maximum peak during each second) was used. This was generally found to underestimate the 100th percentile crest factor by less than 2 dB. The results in Figure 6 suggests that the statement by Gabrielson *et al*. is a reasonable, but perhaps somewhat conservative, estimate. The crest factor ranges between about 12-16.5 dB and is an indicator that is likely sensitive to small variations in the microphone positioning, construction, etc However, despite the noisiness of the map, it is also clear that the crest factor maximum, at least as measured in this experiment, is not associated with the maximum radiation direction, but is generally larger aft of the aircraft It is possible that the crest factor is related to the relative high-frequency content in a signal, which is expected to be greater toward the sideline, but that is only supposition at this point.

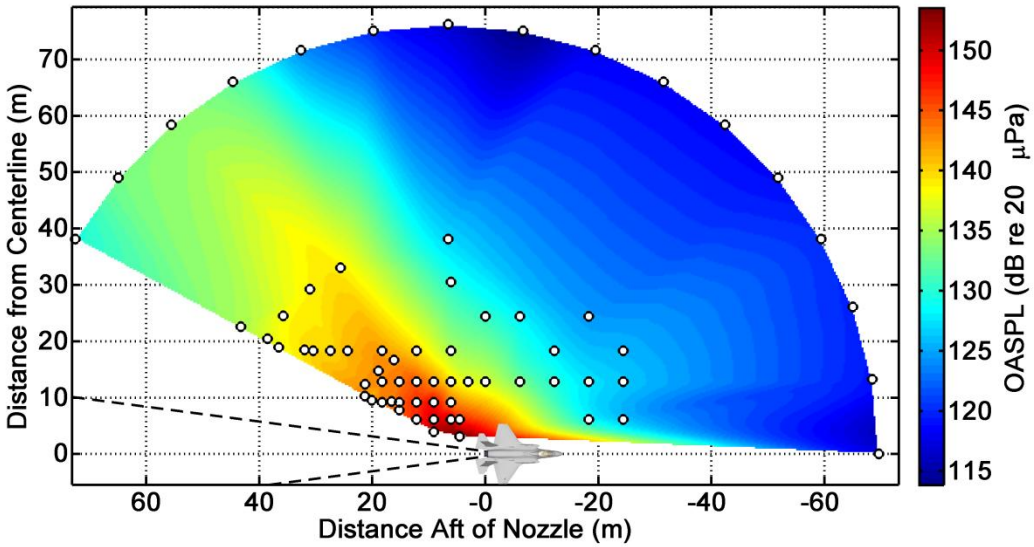

Figure 5. Overall sound pressure level map of the F-35AA at military engine power.

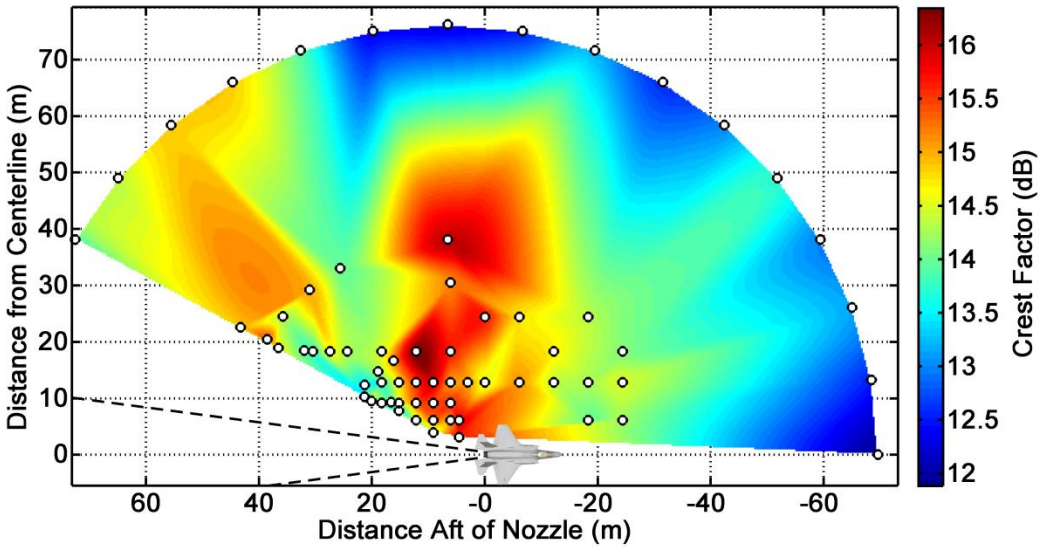

Figure 6. The 99.999th percentile crest factor, in decibels, of the F-35AA at military engine power.

B. Frequency-dependent Level Maps

Corresponding maps of one-third octave band levels are informative. Shown in Figure 7 and Figure 8 are the maps for 200 Hz and 2000 Hz with the aircraft at military power. The 200 Hz frequency is in the vicinity of the peak frequency for maximum radiation direction for this condition. It is clear in comparing the two figures that the lower frequency radiation extends over a broader spatial range, appears to originate farther downstream, and propagates at a slightly shallower angle relative to the jet axis. However, the difference appears to be only about 5°. At 200 Hz, the maximum radiation angle is 130° and, based on the interpolation scheme, it appears to be approximately 125° at 2000 Hz. Forward of the aircraft, the sound radiation is more uniform, but there is greater shielding present at 2000 Hz than at 200 Hz directly in front of the aircraft (0°).

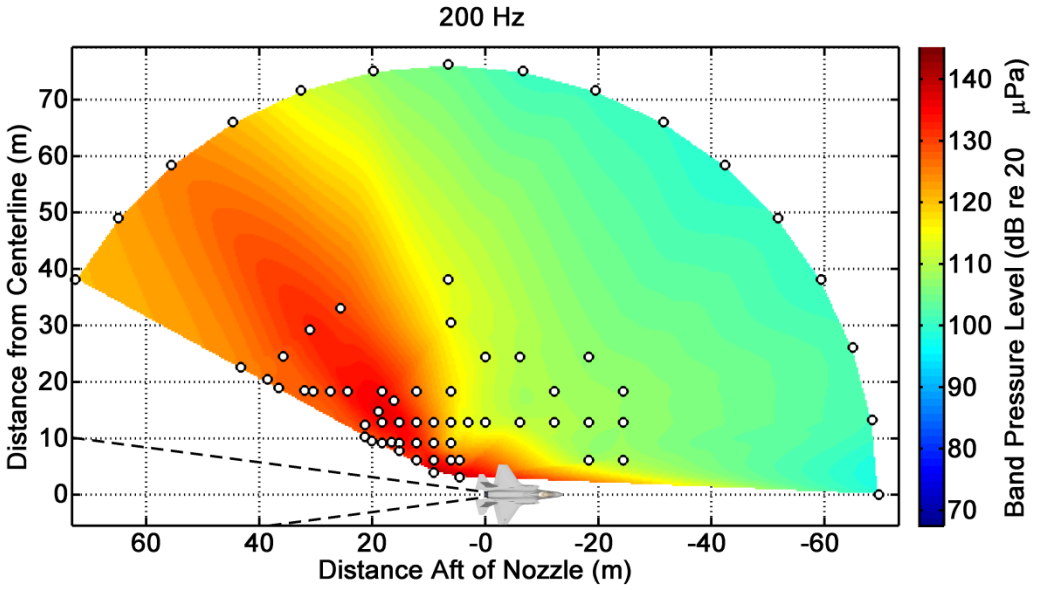

Figure 7. Sound pressure level map of the F-35AA at military engine power and 200 Hz.

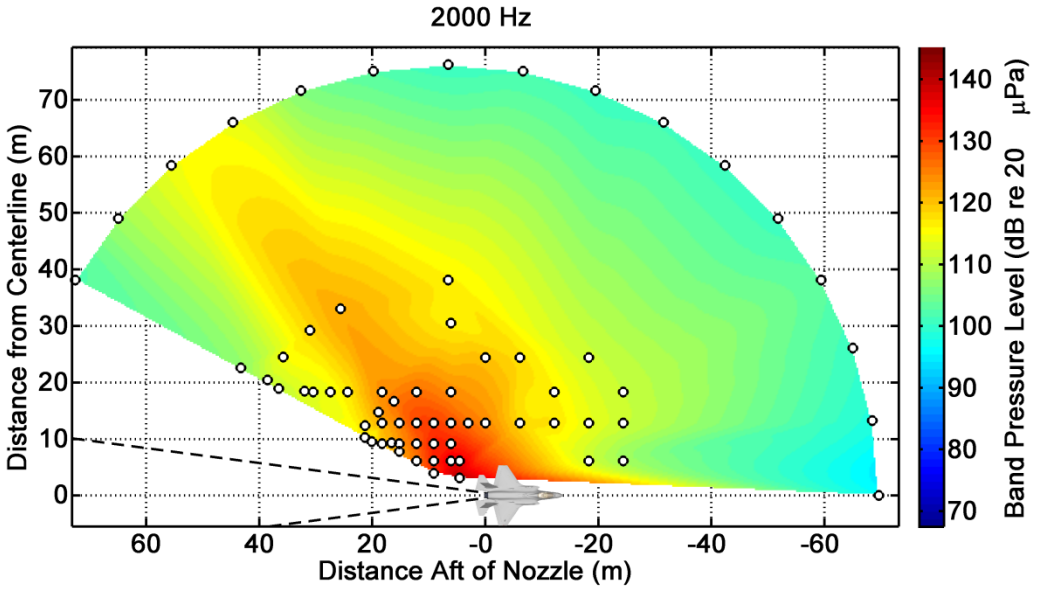

Figure 8. Sound pressure level map of the F-35AA at military engine power and 2000 Hz.

IV. Nonlinear Propagation

The measured levels in Sec. III (~135 dB re 20 μPa at 76 m) suggest the presence of nonlinear effects. An examination of these effects is carried out in two forms. First, a Gol'dberg number analysis is performed. Second,

the measured propagation along the maximum radiation angle of 130° is compared to the results of predicted nonlinear and linear propagation.

A. Gol'dberg Number Analysis

In nonlinear acoustics, the Gol'dberg number, Γ, is the dimensionless ratio between the absorption length, $\ell_a = 1/\alpha$, where α is the absorption coefficient, and the shock formation distance, $\bar{x}$. For $\Gamma \gg 1$, the propagation is highly nonlinear, and for $\Gamma \ll 1$, nonlinear effects can be neglected. Thus, the Gol'dberg number can be a useful measure. The absorption coefficient, α, at frequency, *f*, is readily obtained using standardized equations. based on ambient pressure, temperature, and relative humidity. [14] In considering shock formation distance for noise, however, the analysis is not so straightforward. The shock formation distance refers to the location where the local time derivative of the pressure approaches infinity.

In noise, the random amplitudes cause shock formation to occur at different rates, thus precluding exact analytical treatment. There are, however, two basic approaches considered here, that may provide a qualitative assessment of the likelihood of nonlinearity via Gol'dberg numbers. First, the shock formation distance can be determined analytically for planar and spherical sinusoids. The noise can be decomposed as a function of frequency and the shock formation distance; hence, the Gol'dberg number, for each frequency can be found by treating each frequency component as an independent sinusoid. For a sinusoidal plane wave of frequency, f, and amplitude, P, the shock formation distance may be written as

$$\bar{x} = \frac{\rho_0 c_0^3}{2\pi f \beta P}, \tag{1}$$

where ρ_0 and c_0 are standard density and small-signal sound speed, and β is the coefficient of nonlinearity of the medium ($\beta \approx 1.201$ in air) . The spherical wave shock formation distance may be written in terms of Eq. (1) as

$$\bar{r} = r_0 e^{\bar{x}/r_0}, \tag{2}$$

where $r_0$is the distance at which the sinusoidal amplitude, *P*, is known.

The second approach is to define a characteristic nonlinear distortion length that has the same form as the sinusoidal shock formation distance. Rudenko and Gurbatov[15] express this planar characteristic distortion length as

$$\overline{x_c} = \frac{\rho_0 c_0^3}{2\pi f_c \beta p_{\text{rms}}}, \tag{3}$$

where f_c is the characteristic frequency of the noise and $p_{\text{rms}}$is the root-mean-square pressure. Similar to Eq. (2), we can define a spherical characteristic distortion length as

$$\overline{r_c} = r_0 e^{\overline{x_c}/r_0} \tag{4}$$

Equations (1-4) lead to four definitions for Gol'dberg numbers,

$$\Gamma_P(f) = \ell_a(f)/\bar{x}(f) \tag{5}$$

$$\Gamma_S(f) = \ell_a(f)/[\bar{r}(f) - r_0] \tag{6}$$

$$\Gamma_{c,P} = \ell_a(f_c)/\overline{x_c} \tag{7}$$

and

$$\Gamma_{c,S} = \ell_a(f_c)/[\overline{r_c} - r_0]\,. \tag{8}$$

Equation (8) was examined previously by Gee[16] in the context of scalability of nonlinear propagation as a function of geometric, acoustic, and environmental variables.

Displayed in Figure 9 is the one-third octave band spectrum at 76 m and 130° at military power, along with the four Gol'dberg numbers calculated from Eqs. (4-8). Note that any of the methods neglects the nonlinear propagation that has occurred up to 76 m, but treats solely the amplitudes at that distance. The planar results provide an upper theoretical bound, whereas the spherical results are more realistic, as far as the difference in geometric spreading as a function of frequency are concerned. The Γ_S curve indicates that the Gol'dberg number at any one frequency is rather small, $\Gamma_S \ll 1$, where again, each frequency as an independent sinusoid. This illustrates the danger in estimating nonlinear effects at a single frequency, because as shown in the nonlinear model comparisons below, the nonlinear propagation is appreciable. The $\Gamma_{c,S}$ and $\Gamma_{c,P}$ analyses could be thought of as "integrated" versions of Γ_S and Γ_P, because they use the rms pressure. The fact that $\Gamma_{c,S} > 4$ indicates appreciable nonlinear effects. The characteristic frequency, f_c, was selected to be one one-third octave band higher than the peak frequency in recognition of the fact that there is substantial broadband content above the peak frequeny region. If a greater f_c was chosen, $\Gamma_{c,S}$ would also have been greater. In any event, the spherical characteristic Gol'dberg number analysis shows that nonlinear propagation is non-negligible and is a more useful measure than treating each frequency independently.

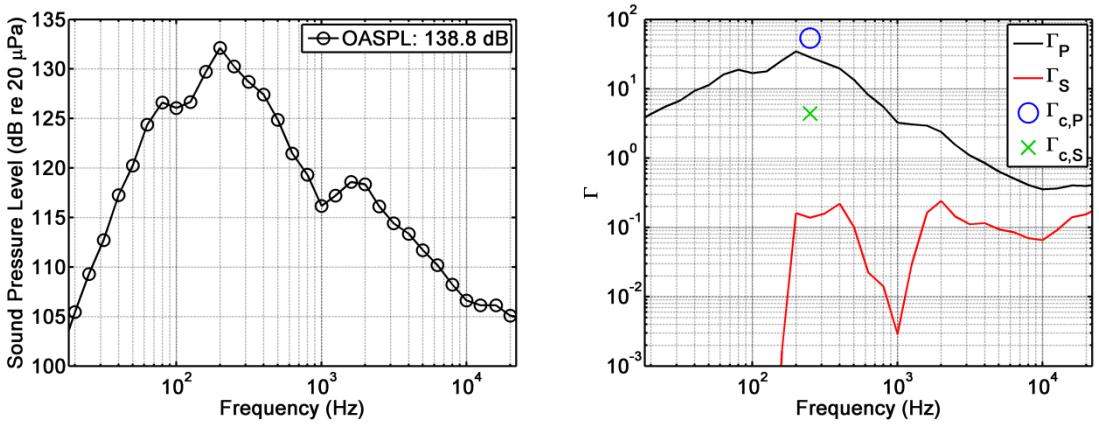

Figure 9. Measured spectrum (left) at 76 m and 130° for the aircraft at military power, and (right), Gol'dberg number analysis of the spectrum.

B. Model Description

The nonlinear propagation model employed is a numerical solution to the generalized Mendousse-Burgers equation (GMBE) for parabolic, spherical propagation through air. The model has been described previously in a number of publications[16-18] and has been used to model nonlinear propagation from a large horn-coupled loudspeaker[18], inside a long cylindrical pipe,[19] and from the F-22A Raptor.[9,10] However, two works[20,21] that employed alternate nonlinear propagation schemes have suggested further study and refinements included here. The basic model employed previously utilizes a waveform as input and then distorts the waveform according to the lossless Earnshaw solution. The waveform is transformed to the frequency domain where geometric spreading and absorption and dispersion are incorporated. To keep the waveform singly valued and at equal time intervals, small spatial steps are taken and a linear interpolation is performed at each step. Choices made in defining step size and the filtering effects of interpolation at shocks lead to some inaccuracies that ultimately have a minor effect on the spectrum, but which can cause erroneous predictions for weakly nonlinear propagation over short ranges.[21]

To explore nonlinear propagation for the F-35 data, the performances of the traditional model has been investigated and three improvements have been made. First, the use of weak-shock theory has been directly implemented, as Pestorius and Blackstock[22] originally suggested with their algorithm. This allows the user to define a minimum desired step size $\Delta x_{\min}$ for spatial regions where weak shocks are present. This step can be significantly larger than the adaptive step size, $\Delta x = \eta \bar{x}$, where $\eta < 1$, which is a fraction of the shock formation distance and keeps the waveform singly valued. In regions where the adaptive step size becomes larger than the minimum weak-shock step size, the step size is allowed to grow. This allows the algorithm to run more efficiently, since step sizes can be made to be on the order of a meter as opposed to millimeters when shocks are present.

The second improvement investigated is the choice of η, in determining the adaptive step size. If η is too small, the steps in the propagation model are too small and lead to interpolation errors, particularly in the case where coarsely sampled shocks are present. It is has been found that a larger step size, $\eta > 0.5$, seems to provide better

results. Significantly better agreement with the model-scale data comparisons of Saxena *et al.*[21] was found if a value of $\eta = 0.9$ was used. Some results detailing the effect of these first two changes in the propagation modeling are shown in the following subsection. It is found that the impact of these changes is generally small for the case considered.

The final improvement is to utilize the suggestion provided by Gee *et al.* in the F-22A Raptor study.[9] The traditional nonlinear model incorporates geometric spreading, atmospheric absorption and dispersion, and quadratic nonlinearity. Ignored are terrain, wind, turbulence, and other effects present in a real outdoor measurement. An empirical approximation to the effects of these environmental factors on the propagation can be obtained by analyzing the measurements taken at idle power. This is convenient because prior to any high-power runup, data are usually taken at idle power. It was found that by 1) finding the difference between the idle measurement and a free-field linear prediction at low and mid frequencies, and 2) applying that empirical correction to the high-power predictions (both linear and nonlinear), the modeled spectra can be improved. Thus the updated model is a numerical solution to the GMBE augmented with weak-shock theory and with other propagation effects taken into account empirically.

C. Nonlinear Propagation Comparisons

Figure 10 shows a small segment of the military power waveform at 76 m and 130° after being nonlinearly propagated using various implementations of the previously described nonlinear model out to 305 m. No empirical correction has been applied in this case. The adaptive step size η has been varied, and weak-shock theory has been explicitly incorporated into the first seven cases, with different values for $\Delta x_{\min}$. Except for the principal shock shown, the results are nearly identical. With weak-shock theory incorporated into the algorithm, the high-amplitude shock travels faster, as interpolation errors are reduced. As step sizes are made smaller, the numerical errors present in the algorithm keep the shock from advancing relative to the rest of the waveform. The first and last cases shown in the legend bound all the results in that they respresent the fastest and slowest traveling shocks.

It is also illustrative to consider the effect of the different iterations on the spectrum. Shown in Figure 11 are one-third octave spectra for the cases considered in Figure 10, but for the entire waveform consisting of 2^{19} samples. Because the only difference between any of the models is at the shocks, predicted spectral differences are manifest most readily at high frequencies. Because numerical implementation leads to slightly different results, this leads to an estimated uncertainty in the numerical model of approximately ± 2 dB at 20 kHz. Note that the three groupings of high-frequency curves follow the choice of η, with $\eta = 0.9$ having the most high-frequency energy and not whether weak-shock theory was used or its minimum step size. The biggest difference among model variations is computational efficiency; the first simulation, with the largest step size, ran in approximately one minute, whereas the last, with the smallest step size and no $\Delta x_{\min}$, took slightly more than an hour on a quad-core, 64-bit machine with 8 GB of RAM.

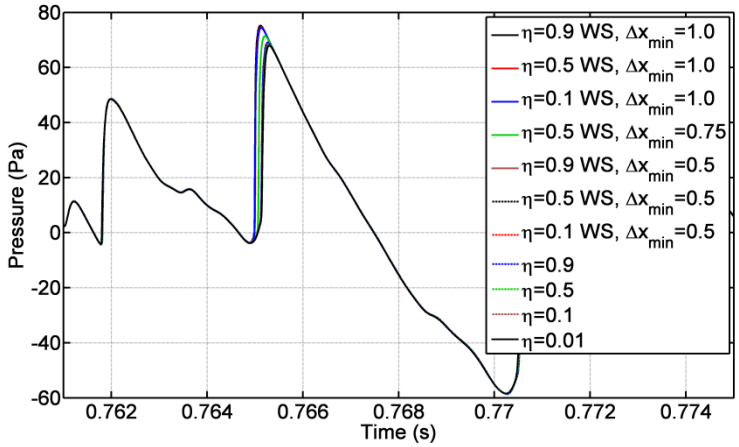

Figure 10. Result of nonlinear propagation model for several different choices of step size with and without weak-shock theory.

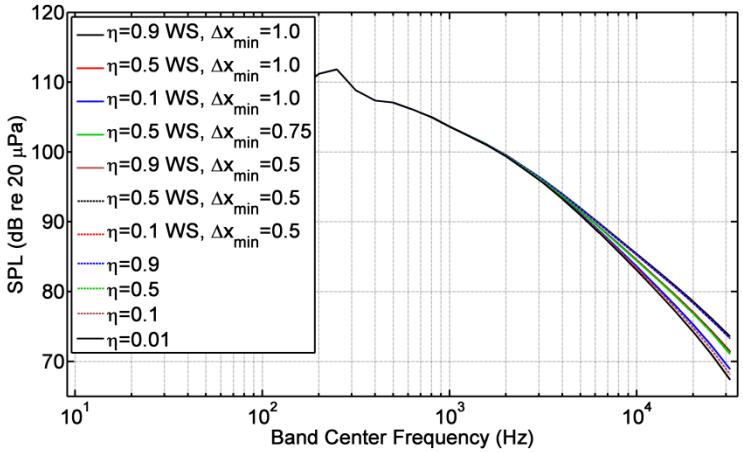

Figure 11. Nonlinearly predicted one-third octave spectra corresponding to Figure 10.

Another interesting case in examining sensitivity of the nonlinear modeling process is to consider the effect of the uncertainty in atmospheric data on nonlinear propagation predicitons. Shown previously in Figure 3 were the differences in level predicted by linear theory based on atmospheric absorption due to changes in relative humidity and temperature. Figure 12 displays the differences in the nonlinear predictions at the extrema of those conditions, plus the prediction at the condition during the time of the military power run-up. Although the behavior is qualitatively similar, in that there is a transition point in level differences between the mid and high frequency regions, the change in predicted level is much smaller than in the linear case. This is because the only high-frequency energy remaining occurs at at the shock-like portions of the waveform. The particulars of the absorption curves matter less at these waveform segments because of the ongoing transfer of energy upward in the spectrum from the nonlinear steepening. Having said that, at greater distances where absorptive effects become more important, the variations shown in Figure 12 likely become larger.

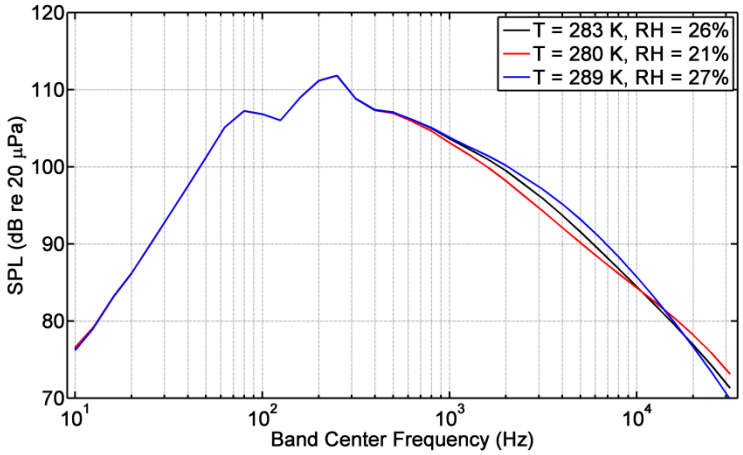

Figure 12. Nonlinear predictions for different atmospheric conditions. The sensitivity of the nonlinear propagation to differences in atmospheric absorption is much less than for the linear case. (See Figure 3).

As described previously, a further improvement to the nonlinear propagation model is to incorporate the other propagation effects empirically, based on a measurement made at idle just before the run-up. Displayed in Figure 13 is the nonlinear propagation prediction with and without the measured empirical correction. The $\eta = 0.5$ WS, $\Delta x_{min} = 0.75$ case from Figure 10 was used because it represents the "average" within the band of uncertainty. The correction boosts the low-frequency levels and reduces the peak levels by a few decibels. The correction was only applied below 2 kHz because of measurement noise floor issues at 305 m for the idle condition.

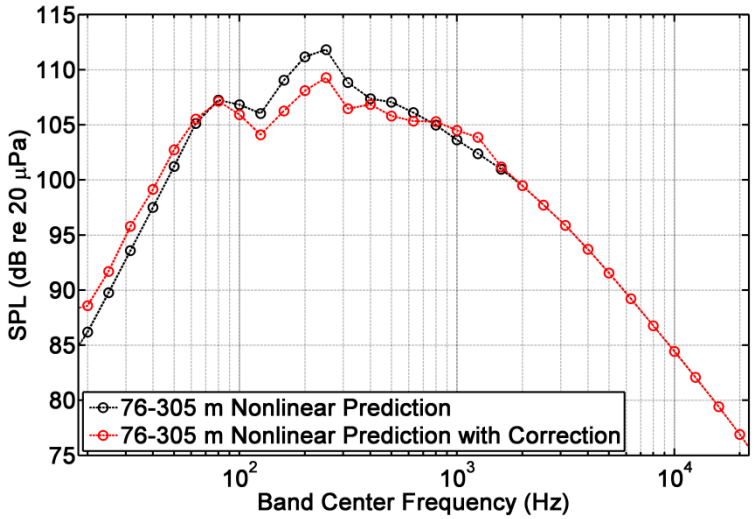

Figure 13. Nonlinear prediction with and without empirical, idle-based propagation difference correction.

The corrected nonlinear spectrum (red) in Figure 13 is shown in Figure 14, along with the (empirically corrected) linear prediction (blue) and the measurement at 305 m (black). The agreement is within 2 dB for any one-third octave band from 20 Hz to 20 kHz. While both the linear and nonlinear predictions match the data extremely well up to 2 kHz, only the nonlinear prediction captures the high-frequency content of the radiated noise. It is noted that the difference between linear and nonlinear propagation predictions above 2 kHz is not as significant as in the previous F-22A Raptor test.[9,10] This is not necessarily to say that the propagation is less nonlinear, but rather says that the atmospheric absorption was less in this measurement, leading to greater linearly predicted levels at high frequencies.

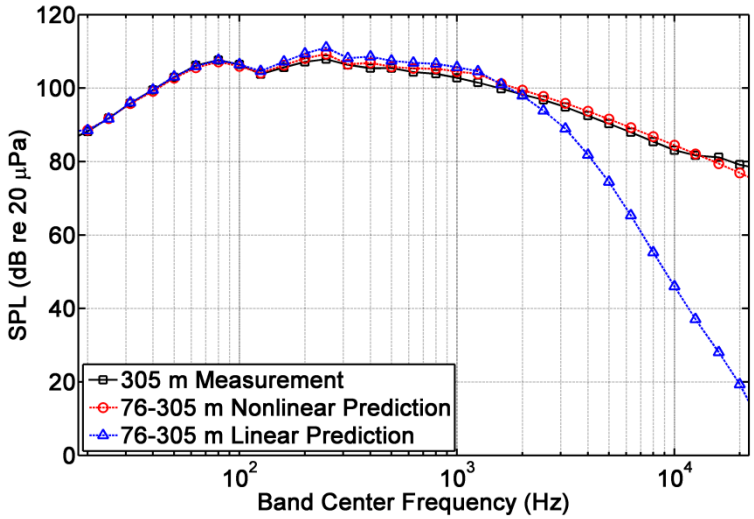

Figure 14. Predicted and measured spectra at 305 m and 130° for the F-35AA at military power.

V. Conclusion

This paper has described some of the details and basic results of the F-35AA ground run-up measurement at Edwards Air Force Base. The characteristic Gol'dberg number analysis qualitatively indicates the presence of nonlinear effects, which have been successfully modeled using a refined version of the generalized Burgers equation solver used previously to model the F-22A propagation. A confirmation of the physics using a second aircraft indicates the utility of such a model and, generally, the prevalence of nonlinearity in the propagation of noise from military jet aircraft.

Acknowledgments

The support of the Joint Strike Fighter Program Office is acknowledged. The authors gratefully acknowledge funding from the Air Force Research Laboratory through the SBIR program and support through a Cooperative Research and Development Agreement (CRADA) between Blue Ridge Research and Consulting, Brigham Young University, and the Air Force. The authors are particularly grateful to Ms. Hilary Gallagher and Ms. Felicia Sexton of the Air Force Research Laboratory for their tireless assistance in helping obtain public release of this paper.

References

[1]Gee, K. L., Petitjean, B. P., McLaughlin, D. K. , and Sparrow, V. W., "Nonlinear Propagation of Noise Radiated from Supersonic Jets," *Proceedings of Noise-Con 04*, edited by C. B. Burroughs and G. C. Maling, Jr., Noise Control Foundation, Poughkeepsie, New York, 2004, pp. 725-733.

[2]Gee, K. L., Gabrielson, T. B., Atchley, A. A., and Sparrow, V. W., "Preliminary Analysis of Nonlinearity in Military Jet Aircraft Noise Propagation, *AIAA Journal* Vol. 43, No. 6, 2005, pp. 1398-1401.

[3]Petitjean, B. P., Viswanathan, K., and McLaughlin, D. K., "Acoustic Pressure Waveforms Measured in High Seed Jet Noise Experiencing Nonlinear Propagation," *International Journal of Aeroacoustics* **5**, No. 2, 2006, 193-215.

[4]Viswanathan, K., "Improved Method for Prediction of Noise from Single Jets," *AIAA Journal* **45**, No. 1, 2007, 151-161.

[5]Viswanathan, K. and Czech, M. J., "Role of Jet Temperature in Correlating Jet Noise," **48**, No. 5, 2009, 1090-1106.

[6]Greska, B. and Krothapalli, A., "On the Far-Field Propagation of High-Speed Jet Noise," *Proceedings of NCAD2008*, paper NCAD2008-73071, July 2008.

[7]Gee, K. L., Atchley, A. A., Falco, L. E., Shepherd, M. R., Ukeiley, L. S., Jansen, B. J., and Seiner, J. M., "Bicoherence Analysis of Model-Scale Jet Noise," *Journal of the Acoustical Society of America*, Vol. 128, No. 5, 2010, pp. EL211-EL216.

[8]Baars, W. J., Tinney, C. E., and Wochner, M. S., "Nonlinear Noise Propagation from a Fully Expanded Mach 3 Jet," AIAA Paper 2012-1177, Jan. 2012.

[9]Gee, K. L., Sparrow, V. W., James, M. M., Downing, J. M., Hobbs, C. M., Gabrielson, T. B., and Atchley, A. A., "Measurement and Prediction of Noise Propagation from a High-power Jet Aircraft," *AIAA Journal* Vol. 45, No. 12, 2007, pp. 3003-3006.

[10]Gee, K. L., Sparrow, V. W., James, M. M., Downing, J. M., Hobbs, C. M., Gabrielson, T. B., and Atchley, A. A., "The Role of Nonlinear Effects in the Propagation of Noise from High-power Jet Aircraft," *Journal of the Acoustical Society of America*, Vol. 123, 2008, pp. 4082-4093.

[11]R. McKinley, R. McKinley, K. L. Gee, T. Pilon, F. Mobley, M. Gillespie, and J. M. Downing, "Measurement of near-field and far-field noise from full scale high performance jet engines," *Proceedings of ASME Turbo Expo 2010*, Glasgow, UK, paper GT2010-22531, June 2010.

[12]Schlinker, R. H., Liljenberg, S. A., Polak, D. R., Post, K. A., Chipman, C. T., and Stern, A. M., "Supersonic Jet Noise Source Characteristics and Propagation: Engine and Model Scale," AIAA paper 2007-3623, May 2007.

[13]Gabrielson, T. B., Marston, T. M., and Atchley, A. A., "Nonlinear Propagation Modeling: Guidelines for Supporting Measurements, *Proceedings of Noise-Con*, Vol. 114, 2005, pp. 275-285.

[14]ANSI, "Calculation of the Absorption of Sound by the Atmosphere," ANSI/ASA S1.26-1995 (R2009).

[15]Gurbatov, S. N. and Rudenko, O. V., "Statistical Phenomena," Chap. 13 in *Nonlinear Acoustics*, edited by M. F. Hamilton and D. T. Blackstock (Academic Press, San Diego, 1998).

[16]Gee, K. L., "Prediction of nonlinear jet noise propagation," Ph.D. Thesis, The Pennsylvania State University, University Park, PA, Aug. 2005.

[17]Gee, K. L., Sparrow, V. S., Gabrielson, T. B., and Atchley, A. A. "Nonlinear modeling of F/A-18E/F noise propagation," AIAA paper 2005-3089, May 2005.

[18]Gee, K. L., Sparrow, V. W., James, M. M., Downing, J. M., and Hobbs, C. M., "Measurement and prediction of nonlinearity in outdoor propagation of periodic signals," *Journal of the Acoustical Society of America*, Vol. 120, 2006, pp. 2491-2499.

[19]Falco, L. E., Gee, K. L., Atchley, A. A., and Sparrow, V. W., "Investigation of a Single-Point Nonlinearity Indicator in One-Dimensional Propagation," Forum Acusticum Paper # 703, Budapest, Aug. 2005.

[20]Wochner, M., "Numerical Simulation of Multi-Dimensional Acoustic Propagation in Air Including the Effects of Molecular Relaxation," Ph.D. Thesis, The Pennsylvania State University, University Park, PA, May 2006.

[21]Saxena, S., Morris, P. J., and Viswanathan, K. "Algorithm for the Nonlinear Propagation of Broadband Jet Noise," *AIAA Journal*, Vol. 47, No. 1, 2009, pp. 186-194.

[22]Pestorius, F. M. and Blackstock, D. T. "Propagation of Finite-Amplitude Noise", *Finite-amplitude wave effects in fluids: Proceedings of the 1973 Symposium*, edited by L. Bjorno, IPC Business Press Ltd, Surrey, England, 1973, pp. 24-29.